Image Based Visual Servoing for Omnidirectional Wheeled Mobile Robots in Voltage Mode

Armando Saenz[1], Victor Santibañez[2], Eusebio Bugarin[3]

[1,2]Tecnológico Nacional de México - Instituto Tecnológico de la Laguna, Blvd. Revolucion y Av. Instituto Tecnologico de La Laguna S/N Torreon Coah., Mexico. CP 27000

[3]Tecnologico Nacional de Mexico - Instituto Tecnologico de Ensenada, Blvd. Tecnologico No. 150, Ex-ejido Chapultepec, 22780 Ensenada, B.C.

Abstract*—This paper presents a new image based visual servoing (IBVS) control scheme for omnidirectional wheeled mobile robots with four swedish wheels. The contribution is the proposal of a scheme that consider the overall dynamic of the system; this means, we put together mechanical and electrical dynamics. The actuators are direct current (DC) motors, which imply that the system input signals are armature voltage applied to DC motors. In our control scheme the PD control law and eye-to-hand camera configuration are used to compute the armature voltages and to measure system states, respectively. Stability proof is performed via Lypunov direct method and LaSalle's invariance principle. Simulation and experimental results were performed in order to validate the theoretical proposal and to show the good performance of the posture errors.*

Keywords—IBVS, posture control, omnidirectional wheeled mobile robot, dynamic actuator, Lyapunov direct method.

I. INTRODUCTION

Wheeled mobile robots (WMR) are robotic systems with free motion in a plane, and they have capacity to reach every position on the same plane. WMR issues are about how to move them, because they may have or not may have limited trajectories to perform. In our case, we are going to study the omnidirectional mobile robots (OMR)[1] whose trajectories are not limited. In a more particular way, it is emphasized in OMR with four swedish wheels [2]. The methodology proposed in [3], was chosen to obtain the dynamic model, together with the direct current (DC) motor equations presented in [4].

In order to acquire WMR posture by means of computer vision, it is possible to implement global vision systems (GVS). The GVS fits in the *intelligent space* concept [5], [6]. An intelligent space is comprised by sensors (e.g. cameras, microphones, ultrasound or laser range finder), computer, actuators and communication devices. The sensors are used to identificate and track the objects in the space and/or to receive orders from operators. The computer acquires information from sensors, performs image processing, computes control law and communicates with actuators. The intelligent space interacts with objects through robotic platforms (e.g. WMR) that provide services like carrying or delivering loads. GVS are used in robotics soccer competitions to acquire the posture of every robot on the playground [7], [8]. So, GVS are a good option to obtain the posture measurement of WMR.

The contribution of our paper is the proposal of a new control scheme to OMR posture control in voltage mode, requiring only vision system measurements. Furthermore, in our control scheme, the DC motors do not require encoders or drivers with current loop or velocity loop. Document is structured as follow. Section 2 presents the problem statement and the dynamic model in image space too. Control law and stability proof is presented in Section 3. Simulation and experimental results are showed in Section 4. Finally, Section 5 shows our conclusions.

II. PROBLEM STATEMENT

First, the dynamic model of the OMR including actuator dynamics is presented. After, camera model (*thin lens*[9]) and camera configuration (*Eye-to-Hand*[10]) are explained.

2.1 Dynamic model

Consider an OMR with a two dimensional cartesian coordinate frame called Σ_W whose center is O_W and its axes are labeled as $W_1$and W_2. These axes describe a plane where the OMR has free motion. OMR posture on the plane is denoted by $\boldsymbol{\xi} = [x\ y\ \theta]^\top$ (seeFig.1).

Let$\dot{\boldsymbol{\xi}} \in \mathbb{R}^{\mathbf{3}}$ and $\ddot{\boldsymbol{\xi}} \in \mathbb{R}^3$are the velocity and acceleration vector of the OMR respectively,$\boldsymbol{u} = [u_1 \quad u_2 \quad u_3 \quad u_4]^\top$ is the armature voltages vector applied to DC motors. The wheels and actuators (DC motors) are labeled as it is depicted in Fig.2. The dynamic model is an Euler-Lagrange system, given by the following state space representation:

$$\frac{d}{dt}\boldsymbol{\xi} = \dot{\boldsymbol{\xi}} \tag{1}$$

$$\frac{d}{dt}M\dot{\boldsymbol{\xi}} = \frac{k_a}{R_a}R_R^W(\theta)E^\top \boldsymbol{u} - C(\dot{\theta})\dot{\boldsymbol{\xi}} - D\dot{\boldsymbol{\xi}} \tag{2}$$

Where $M \in \mathbb{R}^{3\times3}$ is the diagonal positive definite inertia matrix, $C: \mathbb{R} \to \mathbb{R}^{3\times3}$ is the skew-symmetric gyroscopic matrix, $D \in \mathbb{R}^{3\times3}$ is the symmetric damping matrix, $E \in \mathbb{R}^{4\times3}$ is the jacobian matrix, $R_R^W(\theta)$ is the rotation matrix from Σ_R to Σ_W, $R_a \in \mathbb{R}$ is the armature resistance constant and $k_a \in \mathbb{R}$ is the torque constant for each DC motor.

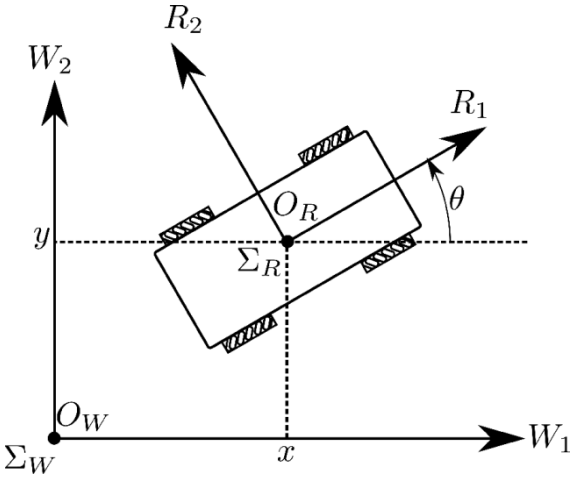

FIG.1: OMR free body diagram

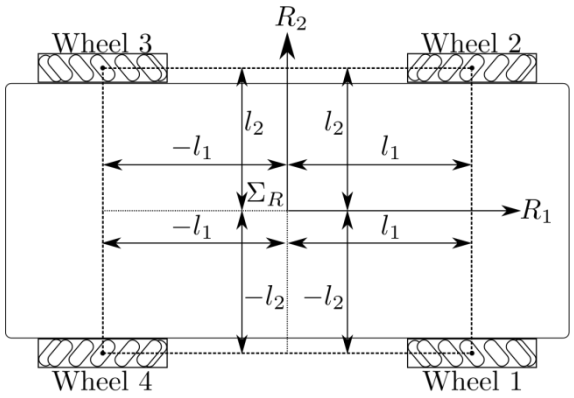

FIG.2: Wheel configuration

2.2 Camera model

Consider the scene depicted in Fig.3. The camera is fixed on the ceiling and oriented to see the robot. The configuration of the camera in Fig.3 is called Eye-to-Hand, in the literature[10]. A photoelectric sensor inside of the camera acquires the scene image. In order to obtain the construction model of the scene image, it is necessary to have the knowledge of *extrinsic parameters* and *intrinsic parameters*. First, the coordinate frame $\Sigma_C$is engaged on the sensor surface, the distance Z_{C3} and angle$\gamma$of $\Sigma_c$respect to Σ_W are the *extrinsic parameters*. Let $\lambda \in \mathbb{R}_+$ be the distance between camera lens and photoelectric sensor, $\alpha_u, \alpha_v \in \mathbb{R}_+$ be the constants that convert from cartesian space to image space. These latter parameters are called: *intrinsic parameters*.

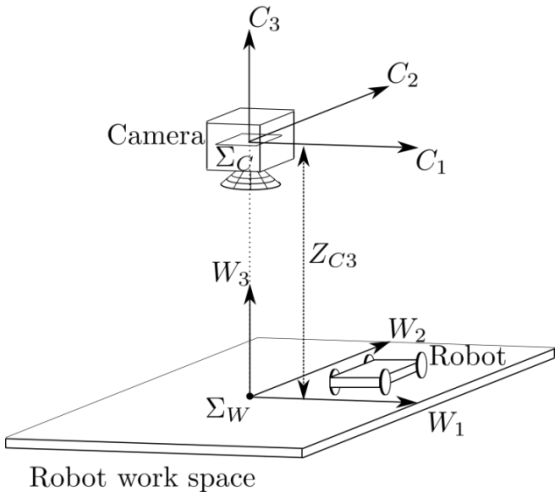

FIG.3: Configuration *Eye-to-Hand*

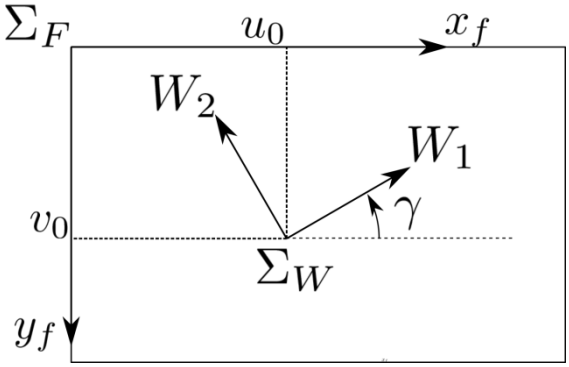

FIG.4: Computer screen

In order to convert from cartesian space to image space (see Fig.4), we define $\boldsymbol{\xi}_f \in \mathbb{R}^3$ forthe OMR posture in image space and it is obtained as follow:

$$\boldsymbol{\xi}_f = \begin{bmatrix} x_f \\ y_f \\ \theta_f \end{bmatrix} = K_C R_W^F(\theta_c) \begin{bmatrix} x \\ y \\ \theta + \gamma \end{bmatrix} \tag{3}$$

With

$$K_c = \begin{bmatrix} \frac{\alpha_u \lambda}{Z_{c3} - \lambda} & 0 & 0 \\ 0 & \frac{\alpha_v \lambda}{Z_{c3} - \lambda} & 0 \\ 0 & 0 & 1 \end{bmatrix}, \qquad R_W^F(\gamma) = \begin{bmatrix} \cos(\gamma) & -\sin(\gamma) & 0 \\ -\sin(\gamma) & -\cos(\gamma) & 0 \\ 0 & 0 & 1 \end{bmatrix}.$$

In order to express the dynamic model (1) and (2) in image space, first and second time derivatives from (3) are computed as follow:

$$\dot{\boldsymbol{\xi}}_f = \begin{bmatrix} \dot{x}_f \\ \dot{y}_f \\ \dot{\theta}_f \end{bmatrix} = K_C R_W^F(\gamma) \dot{\boldsymbol{\xi}}, \qquad \ddot{\boldsymbol{\xi}}_f = \begin{bmatrix} \ddot{x}_f \\ \ddot{y}_f \\ \ddot{\theta}_f \end{bmatrix} = K_C R_W^F(\gamma) \ddot{\boldsymbol{\xi}}. \tag{4}$$

Solving for $\dot{\boldsymbol{\xi}}$y $\ddot{\boldsymbol{\xi}}$, we have

$$\dot{\boldsymbol{\xi}} = K_C^{-1} R_F^W(\gamma) \dot{\boldsymbol{\xi}}_f, \qquad \ddot{\boldsymbol{\xi}} = K_C^{-1} R_F^W(\gamma) \ddot{\boldsymbol{\xi}}_f \tag{5}$$

where $R_F^W(\gamma) = \left(R_W^F(\gamma)\right)^\top$. Pre-multiplying (2) with $R_W^F(\gamma)$and substituting equation (5) the state space representation is rewritten as follows:

$$\frac{d}{dt} \boldsymbol{\xi}_f = \dot{\boldsymbol{\xi}}_f \tag{6}$$

$$\frac{d}{dt} M K_C^{-1} \dot{\boldsymbol{\xi}}_f = \frac{k_a}{R_a} R_R^F(\theta_f) E^\top \boldsymbol{u} - C(\dot{\theta}) K_C^{-1} \dot{\boldsymbol{\xi}}_f - D K_C^{-1} \dot{\boldsymbol{\xi}}_f \tag{7}$$

with

$$R_R^F(\theta_f) = \begin{bmatrix} \cos(\theta_f) & -\sin(\theta_f) & 0 \\ -\sin(\theta_f) & -\cos(\theta_f) & 0 \\ 0 & 0 & 1 \end{bmatrix}.$$

Note that (6) and (7) are the open loop dynamic model of a time invariant system, the input signal $\boldsymbol{u}$ is a vector with the four armature voltage of actuators; and the mechanical, electrical and camera parameters are involved in (7).

III. POSTURE CONTROL

3.1 Controller

Let $\boldsymbol{\xi}_f^* \in \mathbb{R}^3$ be the desired posture vector in image space,$\tilde{\boldsymbol{\xi}}_f \triangleq \boldsymbol{\xi}_f^* - \boldsymbol{\xi}_f$be the posture error vector. The aim of our proposed control scheme is to lead the posture error toward zero (i.e. $\lim_{t\to\infty} \tilde{\boldsymbol{\xi}} = 0$). The proposed control law is given by

$$\boldsymbol{u} = G R_R^F(\theta_f) \left[K_p \tilde{\boldsymbol{\xi}}_f - K_d \dot{\boldsymbol{\xi}}_f\right] \tag{8}$$

with

$$G = \begin{bmatrix} 1 & 1 & 1 \\ 1 & -1 & -1 \\ 1 & 1 & -1 \\ 1 & -1 & 1 \end{bmatrix}, \qquad K_p = \begin{bmatrix} k_{p1} & 0 & 0 \\ 0 & k_{p2} & 0 \\ 0 & 0 & k_{p3} \end{bmatrix}, \qquad K_d = \begin{bmatrix} k_{d1} & 0 & 0 \\ 0 & k_{d2} & 0 \\ 0 & 0 & k_{d3} \end{bmatrix},$$

where $k_{p1}, k_{p2}, k_{p3}, k_{d1}, k_{d2}, k_{d3} \in \mathbb{R}$ are positive gains. Substituting the control law (8) in dynamic model (7) we obtain closed loop dynamics. It is shown as follows

$$\frac{d}{dt}\tilde{\boldsymbol{\xi}}_f = -\dot{\boldsymbol{\xi}}_f \tag{9}$$

$$\frac{d}{dt}MK_C^{-1}\dot{\boldsymbol{\xi}}_f = \Lambda\left[K_p\tilde{\boldsymbol{\xi}}_f - K_d\dot{\boldsymbol{\xi}}_f\right] - C(\dot{\theta})K_C^{-1}\dot{\boldsymbol{\xi}}_f - DK_C^{-1}\dot{\boldsymbol{\xi}}_f \tag{10}$$

With $\Lambda = \frac{k_a}{R_a}R_R^F(\theta_f)E^T G R_R^F(\theta_f) = \frac{k_a}{R_a}E^\top G$ a diagonal positive definite matrix. The closed loop dynamics (9)-(10) has a unique equilibrium in $\tilde{\boldsymbol{\xi}}_{\boldsymbol{f}} = \mathbf{0} \in \mathbb{R}^3$ and $\dot{\boldsymbol{\xi}}_f = \mathbf{0} \in \mathbb{R}^3$.

3.2 Stability proof

The control law (8) is a PD control law to been implemented in over actuated systems (the number of the degree of freedom is lower than the number of actuators or number of control signals). In order to demonstrate stability of the equilibrium, we use the following Lyapunov function candidate

$$V(\tilde{\boldsymbol{\xi}}_f, \dot{\boldsymbol{\xi}}_f) = \frac{1}{2}\dot{\boldsymbol{\xi}}_f^\top MK_C^{-1}\dot{\boldsymbol{\xi}}_f + \frac{1}{2}\tilde{\boldsymbol{\xi}}_f^\top \Lambda K_p \tilde{\boldsymbol{\xi}}_f \tag{11}$$

whose total time derivative along of the trajectories of the closed loop equations (9) and (10) is:

$$\dot{V}(\tilde{\boldsymbol{\xi}}_f, \dot{\boldsymbol{\xi}}_f) = -\dot{\boldsymbol{\xi}}_f^\top(\Lambda K_d + D)\dot{\boldsymbol{\xi}}_f \tag{12}$$

By satisfying the inequality $\Lambda K_d + D > 0$, the equilibrium stability is guaranteed. Thus, in order to study asymptotic stability we can apply the LaSalle's invariance principle [11]. Toward this end, notice that in the set

$$\boldsymbol{S} = \left\{\begin{bmatrix}\tilde{\boldsymbol{\xi}}_f \\ \dot{\boldsymbol{\xi}}_f\end{bmatrix} : \dot{\boldsymbol{V}}(\tilde{\boldsymbol{\xi}}_f, \dot{\boldsymbol{\xi}}_f) = \mathbf{0}\right\} = \{\tilde{\boldsymbol{\xi}}_f \in \mathbb{R}^3 \text{and} \dot{\boldsymbol{\xi}}_f = \mathbf{0} \in \mathbb{R}^{\mathbf{3}}\} \tag{13}$$

the largest invariant set $\overline{\boldsymbol{S}}$ is the origin of the closed loop system (9)-(10); i.e., $\overline{\boldsymbol{S}} = \{\tilde{\boldsymbol{\xi}}_f = \mathbf{0} \in \mathbb{R}^3 \text{and} \dot{\boldsymbol{\xi}}_f = \mathbf{0} \in \mathbb{R}^{\mathbf{3}}\}$. So, in accordance with the Corollary 4.2 of[11](see page 129 of [11]) the equilibrium $\begin{bmatrix}\tilde{\boldsymbol{\xi}}_f & \dot{\boldsymbol{\xi}}_{\boldsymbol{f}}\end{bmatrix}^\top = [\mathbf{0} \quad \mathbf{0}]^\top \in \mathbb{R}^6$ is globally asymptotically stable.

IV. SIMULATIONS AND EXPERIMENTAL RESULTS

Our proposed control scheme is depicted in FIG.5. Simulation was performed in MatLab/Simulink. Used notation and parameter values, are shown in TABLE 1. The dynamic model matrices are as follow:

$$M = \text{diag}\{m_R + 4\,m_{R1},\ m_R + 4\,m_{R1},\ 4\,(m_{R1}l_1^2 + m_{R1}l_2^2 + I_{Rz1}) + I_{Rz}\} + \left(I_{Ry1} + J_m r_e^2\right)E^\top E$$

$$E = \frac{1}{r}\begin{bmatrix}1 & 1 & L\\ 1 & -1 & -L\\ 1 & 1 & -L\\ 1 & -1 & L\end{bmatrix}, \quad C(\dot{\theta}) = \left(\frac{4}{r^2}I_{Ry1} + J_m r_e^2\dot{\theta}\right)B, D = r_e^2\left(\frac{k_a k_b}{R_a} + k_v\right)E^\top E,$$

$$B = \begin{bmatrix}0 & -1 & 0\\ 1 & 0 & 0\\ 0 & 0 & 0\end{bmatrix}, \qquad L = l_1 + l_2\,.$$

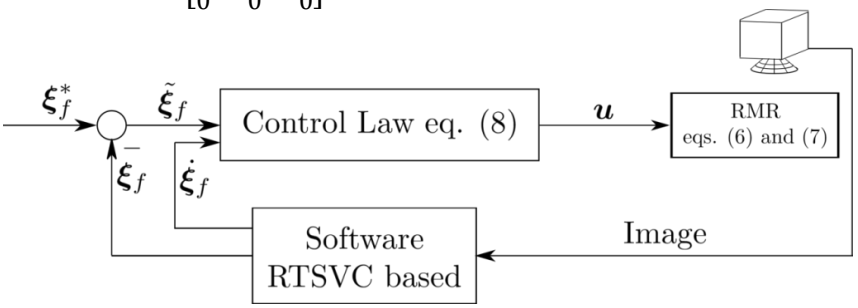

FIG.5: PROPOSED CONTROL SCHEME

Experimental results were performed with a RTSVC based software[12] in order to capture and process the images; the desired posture vector is $\boldsymbol{\xi}_f^* = [43 \quad 53 \quad 0]^\top$ with initial condition given by$\boldsymbol{\xi}_{f0} = [280 \quad 210 \quad 176]^\top$. Gain values are $k_{p1} = 0.5,\ k_{p2} = 0.5,\ k_{p3} = 10.0,\ k_{d1} = 0.005,\ k_{d2} = 0.005$ and $k_{d3} = 1$. The experiment was carried out during 10 seconds with a sample time of 10 milliseconds. Obtained results are depicted in FIG.6, where blue lines are the reference, red lines are the experimental results and green lines are the simulation results. The position (i.e. x_f and y_f) achieves the reference in simulation and experimentation in 1.5 seconds and 3 seconds, respectively. In contrast, the simulation result in orientation (i.e., θ_f) is achieved around 2.5 second and the experimental result has a steady value error reached at 4 seconds, because voltage armature computed by the control law is lower for moving the OMR; this is due to the non-modeled static friction in the DC motor axes. FIG.7 shows the accomplished path, where red dots represent the position of OMR geometric center and green dots represent the position of OMR front part.

TABLE 1
MECHANICAL AND ELECTRICAL PARAMETERS

Parameter	Symbol	Value	Units
Mass of the body	m_R	2.8	Kg
Mass of the wheels	m_{R1}	0.38	Kg
Inertia of the body	I_{Rz}	0.060848	Kg – m^2
Wheels inertia in axis rotor	I_{Ry1}	0.000324	Kg – m^2
Wheels inertial in perpendicular axis rotor	I_{Rz1}	0.000469	Kg – m^2
Distance in R_1	l_1	0.1524	m
Distance in R_2	l_2	0.1505	m
Wheels radius	r	0.42	m
Rotor Inertia	J_m	5.7×10^{-7}	Kg – m^2
Back-EMF Constant	k_b	0.01336	$^{N\,s}/_{rad}$
Torque Constant	k_a	0.0134	$^{N\,m}/_{A}$
Armature resistance	R_a	1.9	Ω
Viscous friction	k_v	0.001	$^{N\,m\,s}/_{rad}$
Gear ratio	r_e	64	1

V. CONCLUSIONS

We have presented a new IBVS scheme for OMR with four swedish wheels. The PD control law was implemented with errors in image space. Stability was proven via Lyapunov direct method, and globally asymptotically stability of the closed loop system was established by using the LaSalle's invariance principle. Positive PD gains of the controller are sufficient to guarantee asymptotic stability in accordance with the stability proof. Simulations show satisfactory results because the states achieved the desired states. Experimental results show a steady state error in the orientation variable, the position reaches to desired position. Steady state error is due to non-modeled static friction in the DC motors axes. As long as, the states are brought closer to desired states, the computed armature voltage by control law decreases. The above implies that the voltage is insufficient to move the remaining angle. A possible solution could be to implement functions like hyperbolic tangent to keep a higher voltage near of desired posture.

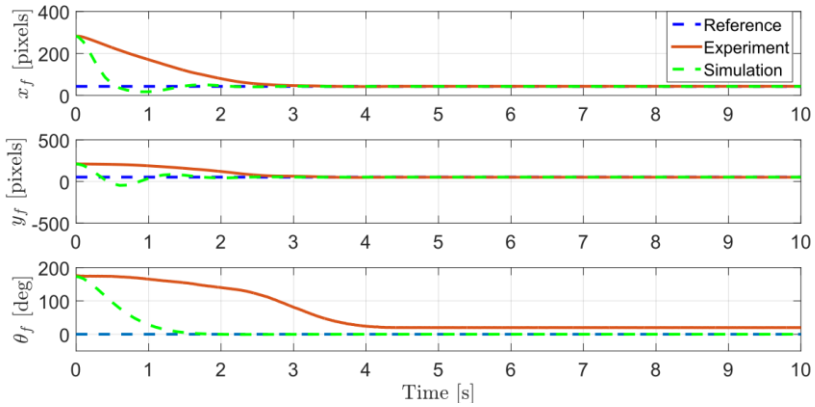

FIG.6: SIMULATION AND EXPERIMENTAL RESULTS

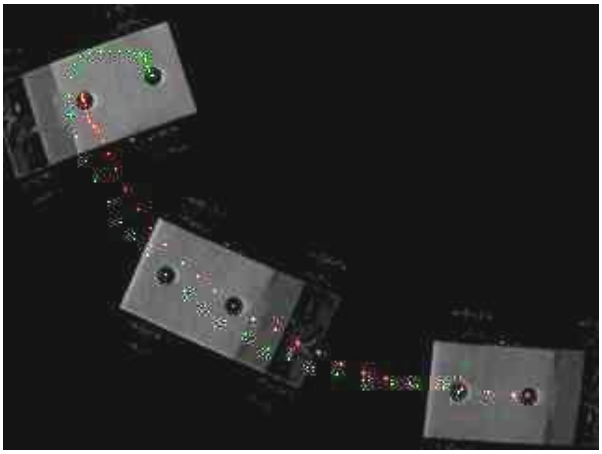

FIG.7 PERFORMED PATH ACQUIRED BY THE CAMERA

ACKNOWLEDGEMENTS

This project has been partially supported by the TecNM, PRODEP and CONACYT 134534 projects.

REFERENCES

[1] K. Watanabe, "Control of an omnidirectional mobile robot," in *Second International conference on Knowledge-Based Intelligent Electronic System*, 1998, no. April, pp. 503–508.

[2] B. E. Ilon, "Wheels for a course stable selfpropelling vehicle movable in any desired direction on the ground or some other base," 3876255, 1972.

[3] G. Campion, G. Bastin, and B. D'Andréa-Novel, "Structural Properties and Classification of Kinematic and Dynamic Models of Wheeled Mobile Robots," *IEEE Trans. Robot. Autom.*, vol. 12, no. 1, pp. 47–62, 1996.

[4] R. Kelly, V. Santibañez, and A. Loría, *Control of Robot Manipulator in Joint Space*. Springer, 2005.

[5] H. Hashimoto, "Present state and future of Intelligent Space - Discussion on the implementation of RT in our environment," *Artif. Life Robot.*, vol. 11, no. 1, pp. 1–7, 2007.

[6] J. H. Lee and H. Hashimoto, "Intelligent space - Concept and contents," *Adv. Robot.*, vol. 16, no. 3, pp. 265–280, 2002.

[7] M. Brezak, I. Petrović, and E. Ivanjko, "Robust and accurate global vision system for real time tracking of multiple mobile robots," *Rob. Auton. Syst.*, vol. 56, no. 3, pp. 213–230, 2008.

[8] M. Brezak and I. Petrovic, "Global Vision Based Tracking of Multiple Mobile Robots in Subpixel Precision," *2007 5th IEEE Int. Conf. Ind. Informatics*, pp. 473–478, 2007.

[9] R. Kelly, "Robust asymptotically stable visual servoing of planar robots," *IEEE Trans. Robot. Autom.*, vol. 12, no. 5, pp. 759–766, 1996.

[10] S. Hutchinson, G. D. D. Hager, and P. I. I. Corke, "A Tutorial on Visual Servo Control," *IEEE Trans. Robot. Autom.*, vol. 12, no. Octubre, pp. 651–670, 1996.

[11] H. K. Khalil, *Nonlinear Systems*, 3a ed. 2002.

[12] E. Bugarin and R. Kelly, "RTSVC: Real-time system for visual control of robots," *Int. J. Imaging Syst. Technol.*, vol. 18, no. 4, pp. 251–256, 2008.